

^{19}F NMR Study of the Equilibria and Dynamics of the $\text{Al}^{3+}/\text{F}^{-}$ System

A. Bodor,[†] I. Tóth,^{*,†} I. Bányai,[‡] Z. Szabó,[§] and G. T. Hefter^{||}

Department of Inorganic and Analytical Chemistry, Lajos Kossuth University (KLTE), H-4010 Debrecen, Pf. 21, Hungary, Department of Physical Chemistry, Lajos Kossuth University (KLTE), H-4010 Debrecen, Pf. 7, Hungary, Inorganic Chemistry, Department of Chemistry, The Royal Institute of Technology (KTH), 100 44 Stockholm, Sweden, and Chemistry Department, Murdoch University, Murdoch WA 6150, Australia

Received October 25, 1999

A careful reinvestigation by high-field ^{19}F NMR (470 MHz) spectroscopy has been made of the $\text{Al}^{3+}/\text{F}^{-}$ system in aqueous solution under carefully controlled conditions of pH, concentration, ionic strength (I), and temperature. The ^{19}F NMR spectra show five distinct signals at 278 K and $I = 0.6$ M (TMACl) which have been attributed to the complexes $\text{AlF}_i^{(3-i)+}(\text{aq})$ with $i \leq 5$. There was no need to invoke $\text{AlF}_i(\text{OH})_j^{(3-i-j)+}$ mixed complexes in the model under our experimental conditions ($\text{pH} \leq 6.5$), nor was any evidence obtained for the formation of $\text{AlF}_6^{3-}(\text{aq})$ at very high ratios of $\text{F}^{-}/\text{Al}^{3+}$. The stepwise equilibrium constants obtained for the complexes by integration of the ^{19}F signals are in good agreement with literature data given the differences in medium and temperature. In $I = 0.6$ M TMACl at 278 K and in $I = 3$ M KCl at 298 K the $\log K_i$ values are 6.42, 5.41, 3.99, 2.50, and 0.84 (for species $i = 1-5$) and 6.35, 5.25, and 4.11 (for species $i = 1-3$), respectively. Disappearance of the ^{19}F NMR signals under certain conditions was shown to be due to precipitation. Certain ^{19}F NMR signals exhibit temperature- and concentration-dependent exchange broadening. Detailed line shape analysis of the spectra and magnetization transfer measurements indicate that the kinetics are dominated by F^{-} exchange rather than complex formation. The detected reactions and their rate constants are $\text{AlF}_2^{2+} + \text{F}^{-} \rightleftharpoons \text{AlF}^+\text{F}^{2+} + \text{F}^{-}$ ($k_{02} = (1.8 \pm 0.3) \times 10^6 \text{ M}^{-1} \text{ s}^{-1}$), $\text{AlF}_3^0 + \text{F}^{-} \rightleftharpoons \text{AlF}_2^+\text{F}^0 + \text{F}^{-}$ ($k_{03} = (3.9 \pm 0.9) \times 10^6 \text{ M}^{-1} \text{ s}^{-1}$), and $\text{AlF}_3^0 + \text{H}^+\text{F} \rightleftharpoons \text{AlF}_2^+\text{F}^0 + \text{HF}$ ($k^{\text{H}03} = (6.6 \pm 0.5) \times 10^4 \text{ M}^{-1} \text{ s}^{-1}$). The rates of these exchange reactions increase markedly with increasing F^{-} substitution. Thus, the reactions of $\text{AlF}_2^{2+}(\text{aq})$ were too inert to be detected even on the T_1 NMR time scale, while some of the reactions of $\text{AlF}_3^0(\text{aq})$ were fast, causing large line broadening. The ligand exchange appears to follow an associative interchange mechanism. The *cis-trans* isomerization of $\text{AlF}_2^+(\text{aq})$, consistent with octahedral geometry for that complex, is slowed sufficiently to be observed at temperatures around 270 K. Difference between the $\text{Al}^{3+}/\text{F}^{-}$ system and the much studied $\text{Al}^{3+}/\text{OH}^{-}$ system are briefly commented on.

1. Introduction

Aluminum is the most abundant metal in the earth's crust. However, aluminum is not an essential element in biological processes. Indeed, soluble Al^{3+} is a well-known toxin to both plants and animals, and it may also be involved in human diseases.¹ As a *hard* metal ion $\text{Al}^{3+}(\text{aq})$ interacts most strongly with *hard* donors, and therefore its complexes with O- and F-donor ligands are very stable. Such species have been shown to be important in the transport of aluminum in both natural waters and biological fluids^{2,3} and are believed to act as "seed" poisons in the Bayer process.⁴ Complexation of Al^{3+} by F^{-} also plays an important role in the Watts–Utley titration; the reaction is normally represented as $\text{Al}(\text{OH})_4^{-} + 6\text{F}^{-} \rightarrow \text{AlF}_6^{3-} + 4\text{OH}^{-}$.

The fluoride complexes of Al^{3+} have been intensively studied. The system is deceptively simple; it is well represented by the formation of a series of complexes, $\text{AlF}_i^{(3-i)+}(\text{aq})$. The values of the stepwise equilibrium constants have been critically reviewed⁵ and are in excellent agreement for the lower order complexes ($i \leq 3$). However, estimates of K_4 vary by an order of magnitude. Despite the existence of higher order fluoroaluminate species in the solid state, there is little evidence⁶ for the existence of complexes with $i \geq 5$ in aqueous solution.

The $\text{Al}^{3+}/\text{F}^{-}$ system has been investigated by NMR spectroscopy on a number of occasions.⁷ For example, a variety of $\text{AlF}_i^{(3-i)+}$ complexes with $i = 1-3$ were reported in water and organic solvents.⁸⁻¹¹ Unfortunately, owing to technological limitations of the times and the inadequate control of important solution parameters, the early NMR work is only of qualitative

* Corresponding author. E-mail: imreth@delfin.klte.hu.

[†] Department of Inorganic and Analytical Chemistry, Lajos Kossuth University (KLTE).

[‡] Department of Physical Chemistry, Lajos Kossuth University (KLTE).

[§] The Royal Institute of Technology (KTH).

^{||} Murdoch University.

- (1) Corain, B.; Bombi, G. G.; Tapparo, A.; Perazzolo, M.; Zatta, P. *Coord. Chem. Rev.* **1996**, *149*, 11.
- (2) Smith, R. W. *Coord. Chem. Rev.* **1996**, *149*, 81.
- (3) (a) Martin, R. B. In *Encyclopedia of Inorganic Chemistry*; King, R. B., Ed.; John Wiley & Sons: Chichester, 1994; Vol. 4, p 2193. (b) Martin, R. B. *Biochem. Biophys. Res. Commun.* **1988**, *155*, 1194.
- (4) *Ullman's Encyclopedia of Industrial Chemistry*, 5th completely revd ed.; VCH Verlag: Weinheim 1985; pp 566–568.

- (5) Bond, A. M.; Hefter, G. T. *Critical Survey of Stability Constants and Related Thermodynamic Data of Fluoride Complexes in Aqueous Solution*; IUPAC Chemical Data Series No. 27; Pergamon: Oxford, 1980.
- (6) Brosset, C.; Orring, J. *Svensk. Kem. Tidskr.* **1943**, *5*, 101.
- (7) Akitt, J. W. *Prog. NMR Spectrosc.* **1989**, *21*, 41.
- (8) Yamazaki, M.; Takeuchi, T. *Kogyo Kagaku Zasshi* **1967**, *70*, 656.
- (9) (a) Buslaev, Y. A.; Petrosyants, S. P. *Koord. Khim.* **1979**, *5*, 163. (b) Petrosyants, S. P.; Buslaev, Y. A. *Koord. Khim.* **1981**, *7*, 907.
- (10) Hass, D.; Petrosyants, S. P.; Buslaev, Y. A.; Hartley, I. *Dokl. Akad. Nauk. SSSR* **1983**, *269*, 380.
- (11) Petrosyants, S. P.; Buslaev, Y. A. *Koord. Khim.* **1986**, *12*, 907.

use. Evidence for the existence of AlF_6^{3-} in 90% H_2O_2 solution has been provided.¹² More recently,¹³ the existence of $\text{AlF}_i^{(3-i)+}(\text{aq})$ with $i = 1$ and 2 was confirmed, but significantly, difficulties were noted in obtaining signals for higher species. These authors attributed other signals to the formation (at $\text{pH} \geq 2$) of mixed $\text{Al}(\text{OH})\text{F}_i^{(2-i)+}$ complexes.

The structural chemistry of Al^{3+} is dominated by the formation of octahedral species. Other geometries, such as the tetrahedral $\text{Al}(\text{OH})_4^-$ in aqueous solution and AlF_4^- in non-aqueous solvents, are also known.^{14,15}

The kinetics of the formation of $\text{AlF}_6^{2+}(\text{aq})$ was studied.^{16,17} On the basis of conventional kinetic measurements¹⁸ (followed by ^{19}F NMR) a reactivity order was proposed toward F^- of $\text{Al}(\text{H}_2\text{O})_6^{3+} \ll \text{Al}(\text{H}_2\text{O})_5\text{F}^{2+} \ll \text{Al}(\text{H}_2\text{O})_4\text{F}_2^+$. No dynamic NMR studies of the $\text{AlF}_i^{(3-i)+}(\text{aq})$ complexes appear to have been made. The temperature dependence of ^{19}F line widths⁸ suggested the presence of exchange reactions. Similar effects were observed recently;¹³ the temperature-dependent line broadening was explained by proton exchange reactions (i.e., between ligated OH^- and H_2O).

A number of questions remain unanswered about the $\text{Al}^{3+}/\text{F}^-$ system. Is there unambiguous evidence for the existence of $\text{AlF}_i^{(3-i)+}(\text{aq})$ with $i > 4$? What are the structures and reaction dynamics of the $\text{AlF}_i^{(3-i)+}(\text{aq})$ species? Accordingly, this paper presents a reinvestigation of the system by ^{19}F NMR spectroscopy under carefully controlled conditions of pH, temperature, and ionic strength.

2. Experimental Section

Chemicals. Sodium fluoride (Merck p.a.) was crystallized from distilled water, dried at 120 °C, and kept in a desiccator. Stock solutions of 0.200 and 0.0500 M were prepared by weight. Tetramethylammonium fluoride (TMAF) stock solution was prepared (1.00 M) from carbonate-free tetramethylammonium hydroxide (TMAOH) solution by adding HF solution to pH 6.0. The TMAOH solution was standardized by pH-metric titration. Aluminum chloride was prepared from 99.9999% purity Al wire (Ajka, Hungary). A weighed quantity of wire was reacted with a stoichiometric quantity of HCl in a Pt boat kept in a glass vessel. As well as acting as a container the Pt served as a catalyst to speed the reaction time to 1 day. The vessel was cooled and protected against the introduction of impurities by allowing the H_2 formed to evolve *via* a gas-washing bottle containing dilute HCl. A stock aluminum solution of 0.400 M, containing a minimum of free acid, was prepared and its concentration checked by EDTA titration. Potassium chloride (Merck p.a.) and tetramethylammonium chloride (TMACl; Aldrich p.a.) were used without further purification. Hydrochloric acid solutions were made by diluting a standard (Merck, Titrisol) or 37% HCl (Merck p.a.) standardized against potassium hydrogen phthalate.

All measurements were made on solutions at ionic strength $I = 3$ M (KCl) or 0.6 M (TMACl), where $I = 0.5\sum z_i^2 c_i$, and z_i and c_i are, respectively, the charge and the molar concentration of the i th ion. Samples for NMR spectroscopy were prepared in polypropylene vessels. Solid KCl (by weight) or TMACl solution (by volume) was added first, followed by solutions of acid, AlCl_3 , D_2O (10% v/v), double-distilled water, and fluoride. The samples were prepared 1 day before the measurement.

(12) Kon'shin, V. V.; Chernyshov, B. N.; Ippolitov, E. G. *Dokl. Akad. Nauk. SSSR* **1984**, 278, 370 (English translation). ^{27}Al and ^{19}F NMR spectra, measured in 90% (not 80%) H_2O_2 at ca. -40 °C, showed coupling consistent with a central Al^{3+} coordinated to six equivalent fluoride ligands, with $^1J_{\text{Al}-\text{F}} = 19$ Hz.

(13) Martinez, E. J.; Girardet, J.-L.; Morat, C. *Inorg. Chem.* **1996**, 35, 706.

(14) Herron, N.; Harlow, R. L.; Thorn, D. L. *Inorg. Chem.* **1993**, 32, 2985.

(15) Herron, N.; Thorn, D. L.; Harlow, R. L.; Davidson, F. *J. Am. Chem. Soc.* **1993**, 115, 3028.

(16) Shurukin, V. V.; Kozlov, Yu. A.; Blochin, V. V.; Mironov, V. E. *Russ. J. Phys. Chem.* **1976**, 50, 145.

(17) Plankey, B. J.; Patterson, H. H. *Inorg. Chem.* **1989**, 28, 4331.

(18) Zbinden, P. Ph.D. Thesis, University of Lausanne, Lausanne, Switzerland, 1994.

Kinetic measurements were performed on samples with $I = 3$ M (KCl) at 298 K with $0.05 \leq c_{\text{H}} \leq 0.4$ M.

pH Measurements. Free hydrogen ion concentrations in solutions of moderate acidity were measured by a HF-resistant combined glass electrode (Ingold, HF-405-60-57) connected to a pH meter and calibrated by the method of Irving *et al.*¹⁹ to give $\text{pH} = -\log [\text{H}^+]$. Equilibrium concentrations of the different species were obtained by integration of the appropriate NMR peaks. Therefore, all stability constants reported in this paper are stoichiometric constants (*cf.* eq 3).

In more acidic samples, because of dissolution of glass from the Ingold electrode, acid concentrations were taken to be those of the added acid. Occasionally, however, the pH had to be measured in acid samples with little or no buffer capacity. In such cases pH was measured *in situ* by monitoring the observed time-averaged ^{19}F NMR shift (δ_{obs}) of the HF/ F^- signal. Providing the proton exchange is rapid, it is readily shown that

$$\text{pH} = \text{p}K_{\text{HF}} - \log [\delta_{\text{F}} - \delta_{\text{obs}}]/[\delta_{\text{obs}} - \delta_{\text{HF}}] \quad (1)$$

where δ_{F} is the chemical shift of F^- in extreme basic solution and δ_{HF} is the chemical shift of HF in the extreme acidic solution. The values of $\text{p}K_{\text{HF}} = 3.32$ ($I = 3$ M (KCl), 298 K) and $\text{p}K_{\text{HF}} = 3.10$ ($I = 0.6$ M (TMACl), 298 K) were determined with $\delta_{\text{HF}} = -43.08$ ppm and $\delta_{\text{F}} = 0.40$ ppm. This method is sensitive to pH change in the pH range corresponding to $\text{p}K_{\text{HF}} \pm 1.9$.

NMR Measurements. ^{19}F NMR spectra were recorded at 470.5 MHz with Bruker DMX500 and DRX500 spectrometers using a 5 mm inverse probehead in locked mode. The samples were introduced into PTFE NMR tubes, which were inserted into conventional 5 mm glass tubes. The temperature of the probehead was checked by the "methanol-thermometer method".²⁰ Typical NMR parameters were flip angle $\sim 30^\circ$ (6–8 μs), pulse repetition time 0.8–1.5 s, spectral window 4250–11800 Hz, and number of scans 64–160. These parameters allowed quantitative integrations to be obtained from the spectra. The chemical shifts are reported in parts per million toward lower frequencies with respect to an aqueous alkaline solution of 0.01 M NaF ($\delta = 0.00$ ppm) as an external standard. Recalculation to the usual CFCl_3 standard can be done, if $\delta_{\text{CFCl}_3} = 0$ ppm and $\delta_{\text{NaF}} = -121.1$ ppm. Magnetization transfer experiments were performed by shaped pulse sequences. Line widths were determined by fitting Lorentzian curves to the signals. All spectral analyses were done using the Bruker WIN-NMR software.

3. Results and Discussion

Assignment of Species. Stepwise formation of $\text{AlF}_i^{(3-i)+}$ species can easily be followed by ^{19}F NMR; however, it is vital that such measurements be performed under carefully controlled conditions of pH, temperature, and ionic strength. Changing $c_{\text{F}}/c_{\text{Al}}$ at constant pH or changing pH at constant $c_{\text{F}}/c_{\text{Al}}$ enables the assignment of chemical shifts to specific complexes. More importantly, the sensitivity of high-field ^{19}F NMR makes possible measurements at concentrations comparable to those used in classical thermodynamic studies.

The lower complexes are easily detected in solutions of high acidity. Figure 1 shows a typical series of spectra at $c_{\text{Al}} = 5$ mM and $c_{\text{F}}/c_{\text{Al}} = 3$ in 3 M KCl solutions at 298 K measured as a function of HCl concentration. Four signals, corresponding to AlF_6^{2+} , AlF_5^+ , AlF_4^0 , and HF, are seen. As expected, the higher the acid concentration, the lower the intensity of the signals of the higher order species. The chemical shift of the "free" fluoride, HF/ F^- , changes slightly at lower acidities due to exchange with the small amounts of unprotonated F^- , but those of the $\text{AlF}_i^{(3-i)+}$ species do not vary significantly. On the other hand, there is a substantial change in the line widths, especially for the AlF_3^0 and HF/ F^- signals.

(19) Irving, H. M.; Miles, M. G.; Pettit, L. P. *Anal. Chim. Acta* **1967**, 38, 475.

(20) Anthony, L. van Geet *Anal. Chem.* **1970**, 42, 679.

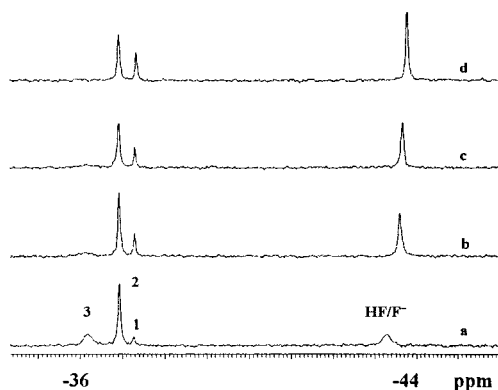


Figure 1. ^{19}F NMR spectra of a solution with $c_{\text{Al}} = 5$ mM, $c_{\text{F}} = 15$ mM, and 3 M KCl at 298 K, at different total acid concentrations, c_{H} : (a) 0.1 M, (b) 0.3 M, (c) 0.4 M, (d) 0.6 M. Numbers 1, 2, and 3 refer to species AlF_2^{2+} , AlF_2^+ , and AlF_3^0 .

An obvious way for detecting higher $\text{AlF}_i^{(3-i)+}$ species is to prepare samples with higher $c_{\text{F}}/c_{\text{Al}}$ ratios and/or at higher pH. Accordingly, c_{F} was varied at constant c_{Al} and with the pH held constant at 4.5 with 0.05 M HAc/Ac^- buffer in 3 M KCl. At $c_{\text{F}}/c_{\text{Al}} \leq 3$ no new signals were detected. Further, at higher ratios, $c_{\text{F}}/c_{\text{Al}} \geq 8$, the signals of the $\text{AlF}_i^{(3-i)+}$ complexes disappeared! This phenomenon was also reported by Martinez *et al.*,¹³ who attributed it to exchange processes. However, as the chemical shift differences for the various $\text{AlF}_i^{(3-i)+}$ species are relatively small, a few parts per million, a complete loss of intensity by broadening seems to be very unlikely. Close inspection of the (semitranslucent plastic) NMR tubes indicated the presence of a fine, colorless precipitate at such concentrations. Analysis by ICP AES of filtered solutions indicated virtually no Al(III) in solution. Dissolution of the solid in 1 M HNO_3 followed by ICP AES accounted for all the “missing” Al(III). The nature of the solid was not investigated further, but AlF_3 , Na_3AlF_6 (and therefore perhaps K_3AlF_6), and a range of $\text{Al}^{3+}/\text{OH}^-/\text{F}^-$ solids are all sparingly soluble in near-neutral aqueous solutions.²¹

Following Brosset and Orring⁶ and others⁹ who reported greater solubilities in R_4N^+ media, a series of solutions were prepared in 0.6 M TMACl (0.05 M HAc/Ac^- buffer) at $\text{pH} \approx 6.0$. No precipitation at $c_{\text{Al}} = 5$ mM occurred, even up to $c_{\text{F}} = 600$ mM. More importantly, at 278 K, in addition to the three signals observed for $\text{AlF}_i^{(3-i)+}$ with $i \leq 3$ in 3 M KCl media at 298 K (Figure 1), two further signals were detected (Figure 2). At low c_{F} (≤ 5 mM), signals 1 (AlF_2^{2+}) and 2 (AlF_2^+) were dominant with minor amounts of signal 3 (AlF_3^0). As c_{F} was increased to 15 mM, signals 1 and 2 progressively decreased, while signal 3 increased along with that of a new signal, 4. At $c_{\text{F}} = 25$ mM ($c_{\text{F}}/c_{\text{Al}} = 5$) signal 4 became dominant, with signal 3 decreasing and a further resonance, 5, beginning to grow. Signal 5 continued to grow up to $c_{\text{F}} = 40$ mM, but remained quite broad. No evidence for a sixth signal was found even up to $c_{\text{F}} = 600$ mM ($c_{\text{F}}/c_{\text{Al}} = 120$). In the absence of excessive line broadening or precipitation, no missing ^{19}F NMR intensity could be detected within the limits of precision of the integration ($\pm 5\%$).^{22b}

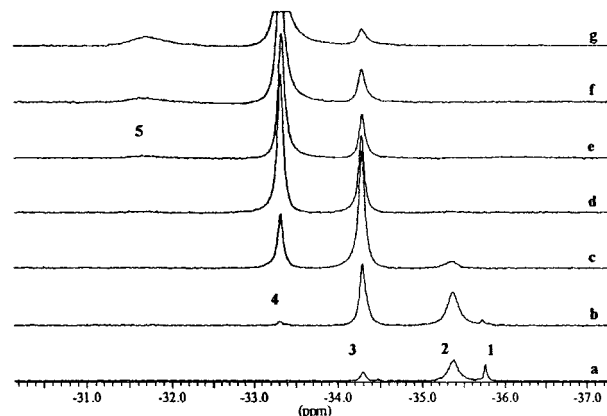


Figure 2. ^{19}F NMR spectra of a solution with $c_{\text{Al}} = 5$ mM, HAc/Ac^- buffer (0.05 M), $\text{pH} \approx 6.1$ and 0.6 M TMACl at 278 K, at different c_{F} values: (a) 5 mM, (b) 10 mM, (c) 15 mM, (d) 20 mM, (e) 25 mM, (f) 30 mM, (g) 40 mM. Numbers 1, 2, 3, 4, and 5 refer to species AlF_2^{2+} , AlF_2^+ , AlF_3^0 , AlF_4^- , and AlF_5^{2-} . The narrow signal of free fluoride at $\delta \approx 0$ ppm is not shown.^{22a}

The most obvious explanation for signals 4 and 5 is to attribute them to the species $\text{AlF}_4^-(\text{aq})$ and $\text{AlF}_5^{2-}(\text{aq})$, respectively. However, at the pH employed (~ 6.0), the formation of ternary $\text{AlF}_i(\text{OH})_j^{(3-i-j)+}(\text{aq})$ species must also be considered. Formation of such complexes is favored at higher pH and modest c_{F} . Accordingly, a series of solutions were prepared in 0.6 M TMACl at $c_{\text{F}}/c_{\text{Al}} = 40/5$ and $20/5$ and $3.7 \leq \text{pH} \leq 6.5$ at 278 K. Typical spectra are shown in Figure S1 of the Supporting Information. The line widths and relative intensities of the signals obtained changed, but the chemical shifts were independent of pH. Thus, ternary complexes do not account for signals 4 and 5, and it is concluded that they can be ascribed to $\text{AlF}_4^-(\text{aq})$ and $\text{AlF}_5^{2-}(\text{aq})$.

The assignments of signals 1–5 and their chemical shifts are summarized in Table 1. The chemical shifts for the lower order complexes ($i \leq 3$) are similar to those of previous studies; quantitative agreement would not be expected given the widely varying concentrations, temperatures, pH, counterions, and chemical shift standards, and the absence of a constant ionic medium in the earlier studies.

Equilibrium Constants. Although NMR spectroscopy does not usually have the precision of potentiometric measurements, it can provide an important independent check on their accuracy. Providing the signal assignments in Table 1 are correct, measurement of the integrated intensities as a function of pH and/or $c_{\text{F}}/c_{\text{Al}}$ enables the stability constants of all detected $\text{AlF}_i^{(3-i)+}(\text{aq})$ species to be determined (see the Supporting Information). The formation of the complexes ($i \geq 1$) can be written as



and the equation of the stepwise stability constants as

$$K_i = [\text{AlF}_i^{(3-i)+}]/[\text{AlF}_{i-1}^{(4-i)+}][\text{F}^-] \quad (3)$$

The values of K_i obtained in this way at 278 K and $I = 0.6$ M (TMACl) and at 298 K and $I = 3$ M (KCl) are summarized in Table 1. Although a detailed comparison with previous data is beyond the scope of the present work, given the differences in the media and the relatively low precision of NMR integrations of broad signals, the agreement with reliable literature values for the lower order complexes ($i \leq 4$) is excellent. Note that

(21) Parthasarathy, N.; Buffle, J.; Haerdi, W. *Can. J. Chem.* **1986**, *64*, 24.

(22) (a) The “slow exchange regime” for $\text{AlF}_i^{(3-i)+}$ and F^- at 278 K turns to “fast exchange” at 298 K, where only one, time-averaged, broad signal of the complexes is detected. Interestingly, the signal of free fluoride remains narrow. Thus, the kinetics of $\text{AlF}_i^{(3-i)+}$ ($i \geq 3$) at higher pH, where these complexes are dominant, could be different from the kinetics discussed below for $\text{AlF}_i^{(3-i)+}$ and HF/F^- . Detailed studies are needed. (b) Hefter, G. T.; Tóth, I.; Bodor, A. Submitted for publication.

Table 1. Equilibrium Constants and Chemical Shift Values of AlF_i⁽³⁻ⁱ⁾⁺ Complexes

signal	assignment	log <i>K_i</i> (lit.) ^a	0.6 M TMACl, 278 K		3 M KCl, 298 K	
			δ (ppm)	log <i>K_i</i> ± est err	δ (ppm)	log <i>K_i</i> ± est err
1	AlF ²⁺	6.11	-35.76	6.42 ± 0.03 (3 points)	-37.27	6.35 ± 0.08 (8 points)
2	AlF ₂ ⁺	4.96	-35.36	5.41 ± 0.09 (7 points)	-36.93	5.25 ± 0.07 (30 points)
3	AlF ₃ ⁰	3.85	-34.29	3.99 ± 0.09 (6 points)	-36.18	4.11 ± 0.12 (7 points)
4	AlF ₄ ⁻	2.35	-33.32	2.50 ± 0.05 (8 points)	<i>b</i>	
5	AlF ₅ ²⁻	1.33	-31.66	0.84 ± 0.20 (9 points)	<i>b</i>	
6	AlF ₆ ³⁻	(0.47)	not detected		<i>b</i>	

^a *I* = 0.5 M (KNO₃), 298 K;⁶ see also refs 5 and 3b. ^b Precipitation occurred.

temperature effects are small (<ca. 0.1 in log *K_i* for a temperature difference of 20 K) on the basis of the known values of Δ*H_i*.⁵

It is interesting and almost certainly significant that the present value of *K₅* (Table 1) is about a factor of 3 lower than the only previous report of this constant. As noted earlier and discussed in detail elsewhere^{22b} no evidence has been obtained for the existence of AlF₆³⁻(aq) at *T* ≥ 255 K and *c_F*/*c_{Al}* ≤ 120 by ¹⁹F NMR. A typical distribution diagram is shown in Figure S2. Note that Al_x(OH)_y^{(3x-y)+} species^{3b} are also included in the model calculation, but they show no contribution to the speciation under our experimental conditions.

Dynamics. As seen from Figure 1 the line widths of the signals except that of AlF²⁺ vary with acidity. With increasing acid concentration the HF signal narrows, whereas those of AlF₂⁺ and AlF₃⁰ broaden. This is a certain indication of the presence of exchange processes. As the number of peaks is equal to the number of species reported by equilibrium studies, the “slow exchange” situation is valid. In this case the line width of the signal for the species *i* (LW_{*i*}) is

$$LW_i = \frac{1}{\pi} \left(\frac{1}{T_{2,i}} + \frac{1}{\tau_{inh}} + \frac{1}{\tau_{ex,i}} \right) \quad (4)$$

where *T_{2,i}* is the transverse relaxation time of species *i*, τ_{inh} the relaxation time due to inhomogeneity of the magnetic field, and τ_{ex,i} the contribution of chemical exchange to the transverse relaxation.

The line broadening of species *i* (LB_{*i*}) resulting from chemical exchange is defined as the difference between the observed line width and the nonexchange line width:

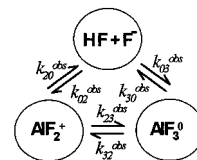
$$LB_i = LW_i - \frac{1}{\pi} \left(\frac{1}{T_{2,i}} + \frac{1}{\tau_{inh}} \right) = \frac{1}{\pi} \sum_{i=0, i \neq j}^n k_{ij}^{obs} = \frac{1}{\pi} k_i^{obs} \quad (5)$$

where *n* is the number of species, *k_{ij}*^{obs} is the pseudo-first-order rate constant of each reaction from site *i* to site *j*, and *k_i*^{obs} is the pseudo-first-order rate constant of all parallel reactions from site *i*. The nonexchange line width is considered to be 12 Hz, which is the line width of AlF₁²⁺, which is proven not to be involved in any exchange processes (*vide infra*). Thus, LB_{*i*} values can be used for kinetic analysis of the system.

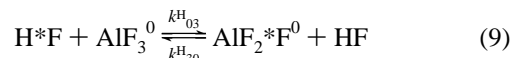
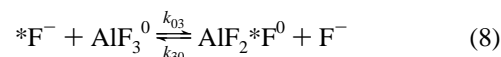
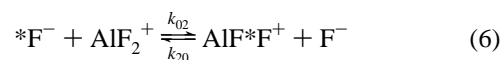
Knowledge of the speciation in the Al³⁺/F⁻ system (*vide supra*) and the analysis of the exchange-broadened spectra show that three sites take part in the exchange process in *I* = 3 M KCl at 298 K. The species AlF²⁺ is excluded, because its line width does not vary with concentration. Therefore, Scheme 1 is an appropriate starting point for the kinetic analysis.

The next step is to find the chemical exchange reactions which can transfer magnetization between the different sites. Three types of such processes are possible. (i) Ligand exchange between the complexes and free ligand (HF and/or F⁻) with no net chemical change (the superscript H indicates exchange with

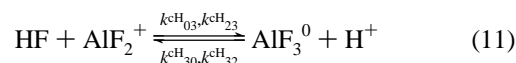
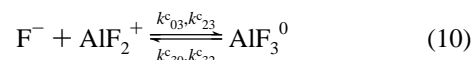
Scheme 1



HF; the subscript *ij* means the magnetization transfer from site *i* to site *j*):



(ii) Complex formation (superscript c or cH):



(iii) Ligand exchange between complexes, “self-exchange”²³ with no net chemical change:



Considering reactions 6–12, we deduced the reaction rates for the various species, using the usual kinetic analysis (see the Supporting Information). The regression analysis of LB_{*i*} vs equilibrium concentration data showed that the following rate equations describe the dynamic system (Figure 3):

$$w_0 = 2k_{02}[AlF_2^+][F^-] + 2k_{03}[AlF_3][F^-] + 2k_{03}^H[AlF_3][HF] \quad (13)$$

$$w_2 = 2k_{20}[AlF_2^+][F^-] \quad (14)$$

$$w_3 = 2k_{30}[AlF_3][F^-] + 2k_{30}^H[AlF_3][HF] \quad (15)$$

These rate expressions indicate that the observed LB_{*i*} are consistent with the occurrence of only three parallel reactions, 6, 8, and 9, with rate constants *k*₀₂ = *k*₂₀ = (8.8 ± 1.4) × 10⁵

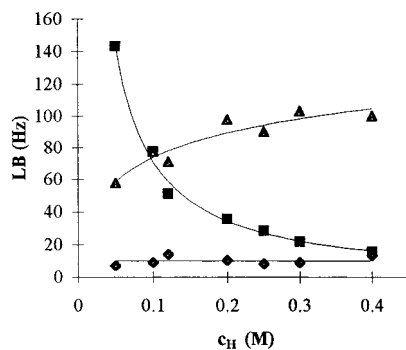


Figure 3. Dependence of line broadening on c_H . The points represent the measured values, while the lines show the calculated values using eqs 13–15 and S19–S21 in the Supporting Information. Symbols ■, ▲, and ◆ refer to species HF/F⁻, AlF₃⁰, and AlF₂⁺, respectively.

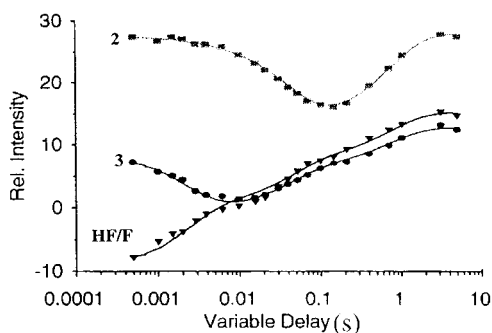


Figure 4. Intensities (arbitrary units) vs delay time (s) for a sample with $c_{Al} = 5$ mM, $c_F = 15$ mM, $c_H = 0.1$ M, and 3 M KCl at 298 K. Numbers 2 and 3 refer to species AlF₂⁺ and AlF₃⁰. Symbols represent measured values.

$M^{-1} s^{-1}$, $k'_{03} = k'_{30} = (1.3 \pm 0.3) \times 10^6 M^{-1} s^{-1}$, $k'_{05} = k'_{30} = (2.2 \pm 0.16) \times 10^4 M^{-1} s^{-1}$. The k' values are the rate constants of a specific²⁴ F⁻ ligand exchange according to the definition $k'_{i0} = k_{i0}/i$. It is notable that all these reactions are symmetrical; i.e., the processes responsible for line broadening are ligand exchange rather than complex formation reactions.

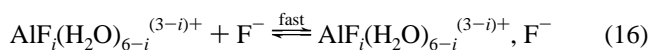
In an attempt to determine the influence of any slower processes, inversion transfer experiments were carried out by selective excitation of each peak, since the longitudinal relaxation time (T_1) is usually longer than the transverse relaxation time (T_2). A typical experiment is shown in Figure 4, where inversion was performed on the HF/F⁻ site. The magnetization transfer to AlF₃⁰ started before the initial observation time, and equilibration between it and HF/F⁻ was complete in 4–5 ms, consistent with the line broadening results. A decrease in the intensity of the AlF₂⁺ signal in the range of 10–100 ms shows that this complex reacts slower than AlF₃⁰. Consistent with the absence of line broadening of the AlF₂⁺ signal, no magnetization transfer was observed to the AlF₂⁺ site, thus fixing an upper rate limit for its exchange processes. The total negative longitudinal magnetization “leaked out” from the system in 2–3 s, illustrating the longer time scale.

The change in longitudinal magnetization with time is described by the matrix equation $\mathbf{M}_\infty - \mathbf{M}_t = \exp(-\mathbf{R}t) \cdot (\mathbf{M}_\infty - \mathbf{M}_0)$. The matrix of pseudo-first-order rate constants (\mathbf{R}) was determined by nonlinear least-squares analysis. Within experimental errors only two rate constants with values $k_{30}^{obs} = 240 \pm 14 s^{-1}$ and $k_{20}^{obs} = 12 \pm 0.2 s^{-1}$ were required to fit

the data. Using eqs 5 and 13–15 and the k'_{ij} values determined from the line broadenings, the pseudo-first-order rate constants were calculated to be $k_{30}^{obs} = 230 s^{-1}$ and $k_{20}^{obs} = 35 s^{-1}$. The agreement between the rate constants obtained from the line broadenings and the magnetization transfer data is excellent for k_{30}^{obs} but is less satisfactory for k_{20}^{obs} . However, it should be remembered that even though the T_1 time scale is more suitable for measuring such slow processes, the magnetization transfer experiments were performed on a single sample, while the line broadening analysis was based on a series of samples.

In summary, the dynamics of the Al³⁺/F⁻ system, at least for AlF₂⁺(aq) and AlF₃⁰(aq) are dominated by fluoride exchange (eqs 6–9) between the complexes and free fluoride (HF/F⁻). Complex formation (water substitution) reactions (eqs 10 and 11) and fluoride exchange between complexes (eq 12) are much slower. Each of these processes will now be considered in detail along with the additional possibility of isomerization.

Fluoride Complexation Processes. In general the ligand substitution reactions of Al³⁺ in aqueous solution are known to follow the I_d mechanism. That is, the rate-determining step (rds) of complex formation is the leaving of a coordinated water molecule from the outer-sphere complex formed in a fast preequilibrium. Thus, for fluoride complexation the mechanism would be expected to be



If the mechanism of complex formation is indeed dissociative in character, the first-order rate constant of the rds, k_{rds} , is expected to be very close to the water exchange rate constant of AlF_{*i*}(H₂O)_{6-*i*}^{(3-*i*)+}. From eqs 16 and 17 $k_{rds} = k/K_{os}$, where the equilibrium constant for eq 16, K_{os} , is usually estimated from one of the Fuoss-type equations.²⁵ Since the water exchange rates are known²⁶ (Table 2), the expected rate constants of the reactions for the formation of AlF₃⁰ from AlF₂⁺ (eqs 10 and 11) can be calculated. For eq 10 this value is $k'_{03} = k'_{23} = 2.4 \times 10^4 M^{-1} s^{-1}$; the value for 11 is even smaller (HF reacts more slowly than F⁻). As these values are considerably smaller than the experimental rate constant ($8.8 \times 10^5 M^{-1} s^{-1}$), this accounts for why complex formation makes no significant contribution to the observed dynamics.

Another way of expressing the relative slowness of the complex formation reactions is to calculate the line broadenings caused by complex formation, assuming they follow the I_d mechanism (eqs 16 and 17). These values, Table 2 (column 5), calculated from the water exchange rate data (also in Table 2) indicate that none of the complex formation reactions contribute significantly to the observed line broadening.

It is interesting to note that an *associative* (I_a) mechanism has been suggested by Plankey and Patterson¹⁷ for the formation of the first complex, AlF(H₂O)₅²⁺, on the basis of the fact that the rate of substitution of H₂O on Al(H₂O)₆³⁺ by F⁻ was greater than that of H₂O exchange, after the application of some statistical corrections. However, this difference was very small.

Fluoride Exchange Processes. A logical starting point to discuss fluoride exchange processes is to assume that they follow

(25) Fuoss, R. M. *J. Am. Chem. Soc.* **1958**, *80*, 5059.

(26) (a) Phillips, B. L.; Casey, W. H.; Crawford, N. S. *Geochim. Cosmochim. Acta* **1997**, *61*, 3041. (b) Phillips, B. L.; Tossell J. A.; Casey W. H. *Environ. Sci. Technol.* **1998**, *32*, 2865.

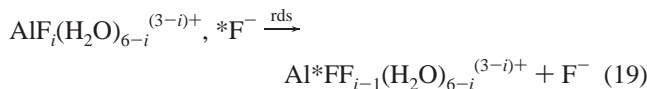
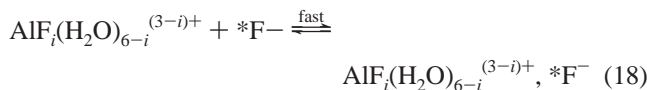
(24) Lincoln, S. F.; Merbach, A. E. In *Substitution Reaction of Solvated Metal Ions*; Sykes, A. G., Ed.; Advances in Inorganic Chemistry Vol. 42; Academic Press: London, 1995; pp 2–78.

Table 2. Rates of Water Exchange k_{ex} (H₂O) and Calculated Values of K_{os} Rate Constants k_{0i}^c , and HF/F⁻ Line Broadenings for Formation Reactions of Various AlF_{*i*}(H₂O)_{6-*i*}^{(3-*i*)⁺} Species

reaction	k_{ex} (H ₂ O) (s ⁻¹) ²⁶	K_{os} (M ⁻¹)	k_{0i}^c (M ⁻¹ s ⁻¹)	LB (Hz) ^a
Al(H ₂ O) ₆ ³⁺ + F ⁻ ⇌ Al(H ₂ O) ₅ F ²⁺	2	20	4 × 10 ¹	< 10 ⁻⁴ , ^b
AlF(H ₂ O) ₅ ²⁺ + F ⁻ ⇌ AlF ₂ (H ₂ O) ₄ ⁺	1 × 10 ²	5	5 × 10 ²	~ 10 ⁻³
AlF ₂ (H ₂ O) ₄ ⁺ + F ⁻ ⇌ AlF ₃ (H ₂ O) ₃ ⁰	2 × 10 ⁴	1.2	2.4 × 10 ⁴	~ 0.1

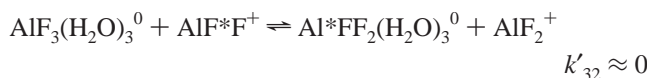
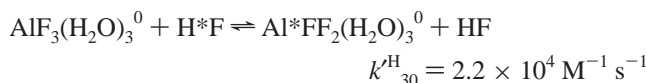
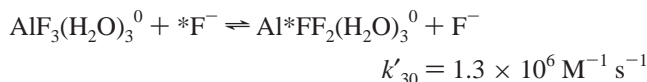
^a Under the conditions of the inversion transfer experiments. ^b The concentration of the Al(H₂O)₆³⁺ complex was estimated from the equilibrium constant.

a mechanism *formally* similar to that of complex formation:

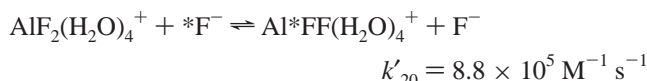


Note, however, this formalism does not indicate whether the rds is dissociative, associative, or concerted.

Comparison of the rate constants for the following three processes



indicates that the rates of fluoride exchange reactions depend dramatically on the nature of the entering group, typical for associative interchange. (Note that as AlF₃⁰ is neutral there is no significant correction to be made for the variation in the charge of the incoming group.) A similar but more limited effect is observed for AlF₂⁺



although here allowance must be made for the difference in charge. Nevertheless, on the basis of these two groups of results, it may be concluded that fluoride exchange reactions are associatively activated.

The occurrence of an I_a mechanism for fluoride exchange is unusual given, as already noted,¹⁷ that most, but possibly not all, Al³⁺ substitution processes follow I_d behavior. According to Lo and Swaddle,²⁷ all substitution processes for octahedral M³⁺ species are I_a unless $r(\text{M}^{3+}) < 0.6 \text{ \AA}$. However, such substitution processes usually refer to the replacement of coordinated H₂O. Since F⁻ is smaller than H₂O and as Al³⁺ is only slightly smaller than 0.6 Å, it is possible that there is sufficient space in the coordination sphere of the Al³⁺ to accommodate an extra (incoming) F⁻. The role of H-bonding is likely to be significant because all of the species under consideration, including HF⁰, are very strongly solvated.

Table 3. Rate Constants of Ligand Exchange Reactions between the Complexes and HF/F⁻

reaction	$k_{0i}, k_{0i}^{\text{H}}$ (M ⁻¹ s ⁻¹) ^b	$k_{\text{rds}} = k_{0i}/K_{\text{os}}$ (s ⁻¹)
AlF ²⁺ + *F ⁻ ⇌ Al*F ²⁺ + F ⁻ ^a	≤ 1 × 10 ⁴ ^c	≤ 2 × 10 ³
AlF ₂ ⁺ + *F ⁻ ⇌ Al*FF ⁺ + F ⁻ ^a	1.8 × 10 ⁶	1.5 × 10 ⁶
AlF ₃ ⁰ + *F ⁻ ⇌ AlF ₂ *F ⁰ + F ⁻	3.9 × 10 ⁶	1.3 × 10 ⁷
AlF ₃ ⁰ + H*F ⇌ AlF ₂ *F ⁰ + HF	6.6 × 10 ⁴	2.2 × 10 ⁵

^a Exchanges of AlF²⁺ with HF/F⁻ and of AlF₂⁺ with HF are too slow to be measured. ^b Exchange constant for partial (unspecified) exchange. ^c Considering the magnetization transfer experiment commented on above, it is observable that in ~3 s the initial situation is reestablished. Therefore, the half-time ($t_{1/2}$) for this experiment is ~0.6 s and $k_{\text{obs}} = (\ln 2)/t_{1/2} \approx 1 \text{ s}^{-1}$. The accuracy of this type of measurement shows that processes which have a first-order rate constant of less than ~0.1 k_{obs} cannot be detected on the T₁ time scale. As the reaction referred to is not detectable, we can calculate an upper limit for k_{01} . The rate equation is $w = 2k_{01}[\text{AlF}^{2+}][\text{F}^-]$ and $k_{\text{obs}} = w/T_{\text{F}} = 2k_{01}([\text{AlF}^{2+}]/1 + k_{\text{HF}}[\text{H}^+])$. Calculating the corresponding concentration values from the spectra, we obtain $k_{01} \leq 10^4 \text{ M}^{-1} \text{ s}^{-1}$.

As the overall reaction embodied in eqs 18 and 19 is unaffected by the nature of the activation in the rds, the rate constants of the rds (eq 19) can be calculated in a manner similar to those for the complexation reactions. The values so obtained are given in Table 3 for those exchange reactions for which the appropriate data are available. Comparison of the rate constants for AlF₂⁺, the only complex for which numerical data are available, for F⁻ exchange (Table 3) with those for water exchange (Table 2) indicate that coordinated fluoride is more labile in these reactions than coordinated water by a factor of about 40, after allowing for the relevant statistical factor. Interestingly, Phillips *et al.* claimed faster water exchange than fluoride exchange, but only reactions 10–12 seemed to be considered. However, similar trends are apparent for both types of bond breaking; i.e., the higher order the complex (the less positive the net charge on the complex), the more labile are both the coordinated F⁻ and water molecules.

It is notable that the present results show that F⁻ exchanges more quickly on AlF_{*i*}^{3-*i*}(aq) than does HF. This is opposite those found for exchange on UO₂F_{*i*}^{(2-*i*)⁺}(aq), the only other system for which F⁻ exchange rates have been measured.²⁸ However, the latter is likely to involve some unusual H-bonding effects. The present order is consistent with the reported rates of *substitution* reactions of F⁻ and HF with both Be²⁺ and Fe³⁺.^{29,30}

Fluoride Exchange between Complexes. Once it is recognized that fluoride exchange processes occur *via* an associative mechanism, then it is readily understood why the exchange of F⁻ between complexes is unimportant on the ¹⁹F NMR time scale. The much greater bulkiness, *cf.* AlF₂⁺ and F⁻ or HF, of an incoming complex inevitably means that in comparison such reactions will be extremely slow.

Isomerization Processes. The temperature dependence of the ¹⁹F NMR spectra suggests another dynamic process in the Al³⁺/

(27) Lo, S. T.; Swaddle, T. W. *Inorg. Chem.* **1975**, *14*, 1878.

(28) Szabó, Z.; Glaser, J.; Grenthe, I. *Inorg. Chem.* **1996**, *35*, 2036.

(29) Baldwin, W. G.; Stranks, D. R. *Aust. J. Chem.* **1968**, *21*, 2161.

(30) Pouli, D.; Smith, W. M. *Can. J. Chem.* **1960**, *38*, 567.

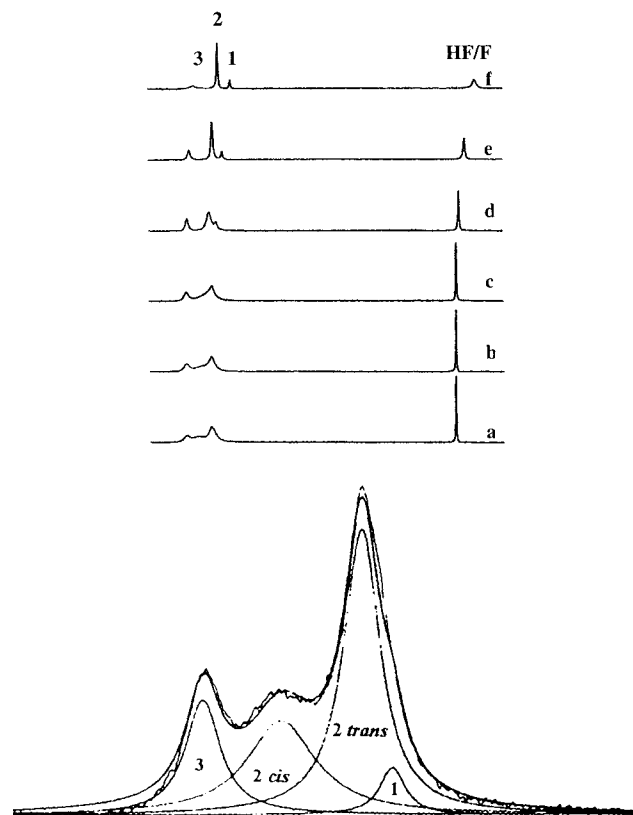
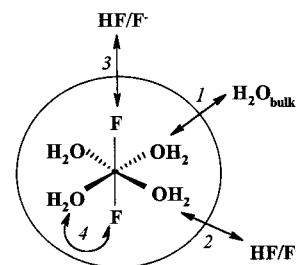


Figure 5. (a, top) ^{19}F NMR spectra of a solution with $c_{\text{Al}} = 5 \text{ mM}$, $c_{\text{F}} = 15 \text{ mM}$, $c_{\text{H}} = 0.1 \text{ M}$, and 3 M KCl at different temperatures, T : (a) 255 K, (b) 259 K, (c) 262 K, (d) 273 K, (e) 287 K, (f) 306 K. Numbers 1, 2, and 3 refer to species AlF_2^{2+} , AlF_2^+ , and AlF_3^0 , respectively. (b, bottom) Band shape analysis for spectra at 255 K from (a). Numbers 1, 2, and 3 refer to species AlF_2^{2+} , AlF_2^+ (*cis* and *trans* isomers), and AlF_3^0 .

F^- system. Selected spectra are shown in Figure 5a. At near ambient temperatures, broadened signals of HF and its exchange partners AlF_3^0 and AlF_2^+ indicate ligand exchange processes between the free and coordinated ligands (see above). Lowering the temperature causes the HF signal to narrow, until at $\sim 262 \text{ K}$ its half-width becomes constant. The explanation for this temperature dependence is the lowered rate of exchange between HF and $\text{AlF}_3^0/\text{AlF}_2^+$; i.e., the intermolecular exchange becomes frozen on the T_2 time scale. (The chemical shift also shows some temperature dependence toward lower fields.) A similar decrease is expected for the line widths of the other sites, AlF_3^0 and AlF_2^+ , involved in the exchange. In fact, these peaks do start to narrow as the temperature is lowered from 306 to 298 K (not shown), but they broaden again at $T < 287 \text{ K}$.

Although it is not obvious from the raw ^{19}F spectra (Figure 5a), band shape analysis (Figure 5b) indicates that signal 2 (AlF_2^+) splits in two at $T < 265 \text{ K}$. Signal 1 almost disappeared under the envelope of signal 2 but is revealed by the numerical analysis, with its correct intensity. The signals become slightly narrower with decreasing temperature to the freezing point of the solutions, $\sim 253 \text{ K}$. The most plausible explanation of the splitting of signal 2 is that the exchange between the *cis*- and *trans*- AlF_2^+ complexes enters into the slow exchange regime on the NMR time scale with decreasing temperature. If it is assumed that the *trans* isomer is favored because of its more symmetrical charge distribution, then the *cis/trans* ratio of the AlF_2^+ isomers at 255 K, estimated from the deconvolution shown in Figure 5b, is approximately 2:1. The line width of signal 3 shows a dependence on temperature broadly similar to that of signal 2. However, as the reactions of AlF_3^0 are faster

Scheme 2



than those of AlF_2^+ , signals for the *mer*- and *fac*- AlF_3^0 isomers cannot be separated under our experimental conditions.

Given that the present NMR measurements indicate that the free ligand (HF/F^-) is not involved in the isomerization reaction of AlF_2^+ (and very likely also not for AlF_3^0 either) at lower temperatures, the probable isomerization mechanism is an *intramolecular* process rather than an *intermolecular* ligand exchange reaction. The NMR measurements indicate that the temperature dependence for the intra- and intermolecular fluoride exchange processes are different; indeed this difference allows their separation.

In summary, the different exchange processes proposed for the $\text{AlF}_i^{(3-i)+}(\text{aq})$ complexes are illustrated in Scheme 2 for $\text{AlF}_2^-(\text{H}_2\text{O})_4^+$. The water exchange process (1) cannot of course be detected by ^{19}F NMR. (However, ^{17}O NMR data are available.²⁶) Further, the complex formation reactions (2) and the exchange reactions of AlF_2^+ are too slow to study by NMR. The rates of ligand exchange (3) between free fluoride (HF/F^-) and AlF_2^+ or AlF_3^0 are faster and fall within the ^{19}F NMR time scale. The isomerization (4) is an intramolecular process.

Geometry of the Complexes. The existence of *cis* and *trans* isomers of $\text{AlF}_2^+(\text{aq})$ is a straightforward proof of its octahedral geometry and thus by implication that of $\text{AlF}_2^+(\text{aq})$ too. It has often been assumed by extension that this must also be true for the higher order complexes ($i \geq 3$). On the other hand, as noted earlier, complexes with geometries other than octahedral certainly exist in the solid state, in melts, and in some *nonaqueous* solutions. Our measurements, like those of previous NMR investigations, do not provide direct information on this matter. Thus, although the observed broadening of signal 3 implies their existence, the *mer* and *fac* isomers of $\text{AlF}_3^0(\text{aq})$ could not be positively identified under our experimental conditions. Similarly, while the existence of $\text{AlF}_5^{2-}(\text{aq})$ implies octahedral geometry, failure to detect AlF_6^{3-} suggests that hasty conclusions on this subject may not be wise. Nevertheless, the constant chemical shift and intensity of ^{27}Al NMR signals, found previously^{13,26b} and measured in this study at different $c_{\text{F}}/c_{\text{Al}}$ ratios (see Figure 2 caption), also support an unchanged geometry for the higher complexes.

Comparison of the $\text{Al}^{3+}/\text{F}^-$ and $\text{Al}^{3+}/\text{OH}^-$ Systems. It is interesting to contrast the behavior of the $\text{Al}^{3+}/\text{F}^-$ system with that of the industrially important $\text{Al}^{3+}/\text{OH}^-$ system. Although unambiguous proof is not as readily available as commonly supposed, a variety of measurements indicate that $\text{Al}(\text{OH})_4^-(\text{aq})$ is tetrahedral.^{31a} Given that OH^- and F^- are isoelectronic and isochoric and show many parallelisms in their chemistry, in both the solution and solid states, it is somewhat surprising that their interaction with $\text{Al}^{3+}(\text{aq})$ should be so dissimilar. As noted by

(31) (a) Watling, H. R.; Sipos, P.; Byrne, L.; Hefter, G. T.; May, P. M. *Appl. Spectrosc.* **1999**, *53*, 415. (b) Watling, H. R.; Fleming, S. D.; von Bronswijk, W.; Rohl, A. L. *J. Chem. Soc., Dalton Trans.* **1998**, 3911.

Tuck³² this is a reflection of the very fine balance among the strengths of interaction of Al^{3+} with the three hard donor ligands H_2O , OH^- , and F^- .

The values of $\log K_i(\text{AlF}_i^{(3-i)+})$ show the normal regular decrease with increasing i (Table 1), which is *circumstantial* evidence for the preservation of octahedral geometry in this series of complexes. In contrast, the values of $\log K_i(\text{Al}(\text{OH})_i^{(3-i)+})$ are 9.0, 8.7, 8.2, and 6.4 for $i = 1-4$, respectively.³³ This lack of variation has been noted by many authors and has been used as evidence of a change in geometry from the octahedral $\text{Al}(\text{H}_2\text{O})_6^{3+}(\text{aq})$ to tetrahedral $\text{Al}(\text{OH})_4^-(\text{aq})$. Where this change occurs is unknown because of experimental difficulties associated with solubility and polymer formation. This dissimilarity

continues for the higher order complexes. Thus, $\text{Al}(\text{OH})_6^{3-}(\text{aq})$ exists but only at very high concentrations (>10 M) of OH^- .^{31b,34} No reliable evidence for $\text{Al}(\text{OH})_5^{2-}(\text{aq})$ exists. In contrast, as shown in this paper, $\text{AlF}_5^{2-}(\text{aq})$ forms readily, yet $\text{AlF}_6^{3-}(\text{aq})$ remains unproven.

Acknowledgment. We thank Dr. Mihály Braun for ICP measurements and the Hungarian National Science Research Foundation (OTKA), Project T 026115, for financial support.

Supporting Information Available: Text describing the determination of the stability constants from ^{19}F integral values and analysis of kinetic data and figures showing ^{19}F NMR spectra, typical distribution diagrams for the Al- and F-fractions, and ^{19}F NMR serial plot of a magnetization transfer experiment. This material is available free of charge via the Internet at <http://pubs.acs.org>.

IC991248W

(32) Tuck, D. G. In *Chemistry of Aluminium, Gallium, Indium and Thallium*; Downs, A. J., Ed.; Blackie Academic & Professional: London, 1993; p 430.

(33) Baes, C. F.; Mesmer, R. E. *The Hydrolysis of Cations*; Wiley: New York, 1976; p 112.

(34) Sipos P.; May, P. M.; Hefter, G. T. To be published.